Chemical Science

ROYAL SOCIETY OF CHEMISTRY

EDGE ARTICLE

View Article Online
View Journal | View Issue

Check for updates

Cite this: *Chem. Sci.*, 2024, **15**, 18818

All publication charges for this article have been paid for by the Royal Society of Chemistry

Received 26th July 2024
Accepted 9th October 2024

DOI: 10.1039/d4sc04990j

rsc.li/chemical-science

Chiral ionic organic single-crystal and its exfoliated two-dimensional nanosheets with enhanced enantioseparation†

Huifeng Liu,[ab] Yongrui He,[c] Jia Chen, *[a] Xiaoqing Qu,[ab] Jing He,[a] Xuwei Chen, *[b] Jianhua Wang [b] and Hongdeng Qiu *[ad]

A chiral ionic organic single-crystal (CIOC) was prepared for the first time through ionic self-assembly using bipyridium chiral ionic liquid (CIL) and 4,4′-biphenyldisulfonic acid (BDA). The CIOC can be ultrasonically exfoliated to produce two-dimensional nanosheets (2D-NSs). The 2D-NSs presented enhanced enantioseparation compared to the CIOC and CIL when used as gas chromatography stationary phase, which may be due to the exfoliated 2D-NSs exhibiting greater exposure of functional groups. Additionally, better resolution of other organic compounds such as positional isomers, *n*-alkanes and *n*-alkanols, Grob mixture, phenols and anilines was obtained in 2D-NSs than CIOC and CIL. This work not only provides a reference for the preparation of chiral ionic organic single-crystals and two-dimensional nanosheets for chiral separation, but also stimulates the preparation of such new ionic organic single-crystals *via* self-assembly for other potential applications.

Introduction

Chiral compounds with two configurations frequently have distinct or even diametrically opposed effects, which makes separating the racemates crucial.[1–3] The similar physicochemical properties of enantiomers results in considerable challenges for their separation.[4–8] Gas chromatography (GC) plays a critical role in the analysis and detection of samples[9,10] due to notable advantages such as minimal sample consumption, rapid detection, and high detection sensitivity.[11–13] The effectiveness of gas chromatography in separating chiral compounds mainly depends on the type and structure of the chiral stationary phase (CSP),[14–17] for which cyclodextrins and their derivatives,[18–20] polysaccharides and their derivatives,[21–23] chiral ionic liquids (CILs),[24,25] pillar[*n*]arene,[26,27] porous organic materials,[28–38] *etc.* are widely utilized.

Of the above materials, ionic liquids possess some specific advantages such as negligible vapor pressure, high thermal stability, and strong polarity,[39,40] and remain a focus for study in numerous domains at present.[41,42] In 2004, CIL as stationary phase was first applied in gas chromatography by Armstrong *et al.*[43] and then attracted much attention.[44,45] Research into framework-materials based on ionic bonding has sparked our interest in ionic materials,[46] however, as far as we know, there have been no reports on the preparation of chiral ionic organic single-crystals (CIOCs) and their application in chiral separation.

In this work, the synthesis of CIOC by the ionic self-assembly of a bipyridium-type CIL with 4,4′-biphenyldisulfonic acid (BDA) was proposed. It is known that 2D nanomaterials always possess the advantages of large surface area, strong interaction between host and guest, *etc.*, which will improve the enantiomeric separation.[47–49] Fittingly, this CIOC can be ultrasonically exfoliated to produce two-dimensional nanosheets (2D-NSs). Interestingly, the 2D-NSs exhibit the best performance when used as GC stationary phase for chiral separation. To the best of our knowledge, this is the first example of chiral ionic-organic single crystal material and the use of its 2D-NSs as CSP material for high-resolution gas chromatographic separation (Scheme 1).

Results and discussion

Preparation of CIL, CIOC and 2D-NSs

The synthesis and characterization of the CIL are shown in the ESI (Fig. S1 and S2).† Equivalent CIL and BDA were dissolved in a mixed solvent of methanol and toluene with heating, and then naturally cooled for recrystallization, and light-yellow transparent crystals were obtained as CIOC with a yield of 39.3%.

[a]*Key Laboratory for Natural Medicine of Gansu Province, Lanzhou Institute of Chemical Physics, Chinese Academy of Sciences, Lanzhou 730000, China. E-mail: jiachen@licp.cas.cn*

[b]*Department of Chemistry, College of Sciences, Northeastern University, Shenyang 110819, China. E-mail: chenxuwei@mail.neu.edu.cn*

[c]*School of Pharmacy, Shandong Second Medical University, Weifang 261053, China*

[d]*Key Laboratory of Rare Earths, Ganjiang Innovation Academy, Chinese Academy of Sciences, Ganzhou 341000, China. E-mail: hdqiu@licp.cas.cn*

† Electronic supplementary information (ESI) available. CCDC 2361107. For ESI and crystallographic data in CIF or other electronic format see DOI: https://doi.org/10.1039/d4sc04990j

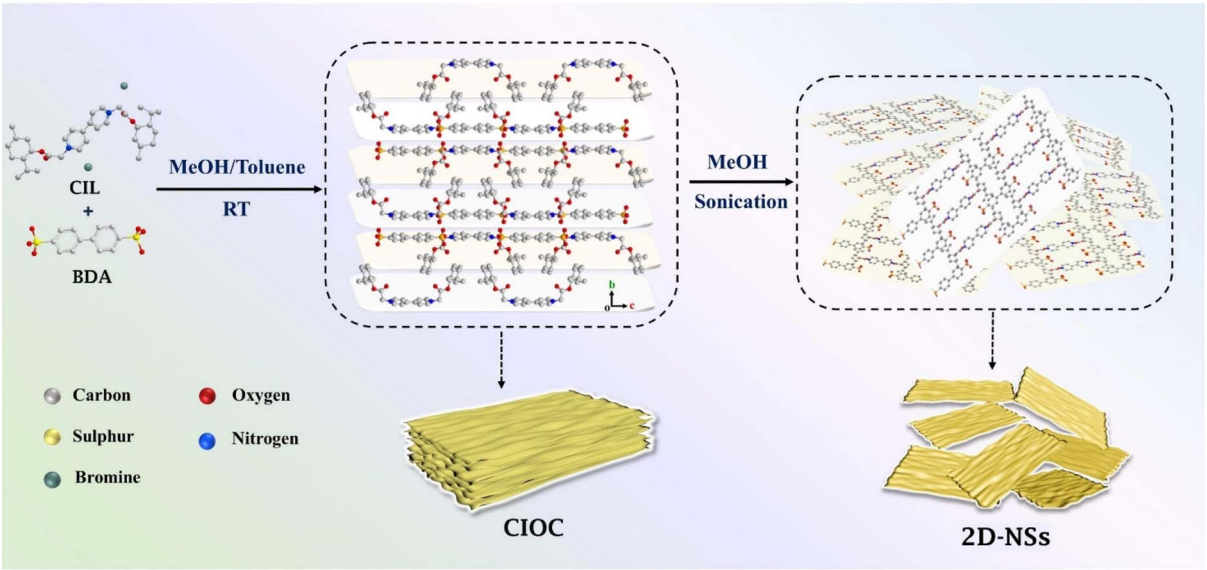

Scheme 1 Synthesis of the chiral ionic organic single-crystal and two-dimensional nanosheets (viewed from the *b* axis).

Then, the CIOC was dispersed in methanol and ultrasonicated for 14 h, resulting in the formation of 2D-NSs.

Preparation of capillary columns

CIL, CIOC and 2D-NSs were coated on the capillary columns (10 m × 0.25 mm i.d.) using the sol–gel method. The detailed method can be found in the ESI.†

Characterization of CIOC and 2D-NSs

Single crystal X-ray diffraction (SXRD) provided detailed chemical composition and bonding information for the CIOC (Tables S1 and S2†), and the crystallographic data (CCDC no. 2361107) showed that the CIOC has the $C222_1$ space group with a = 9.0954 Å, b = 228.981 Å, c = 20.898 Å, and $\alpha = \beta = \gamma = 90°$. The cations and anions are intertwined with each other through the ionic bonds between the positive bipyridium N atoms on the CIL and the negative sulfamic O atoms on the BDA, and each ion is surrounded by four ions of opposite charge on the *bc* planes, combining in the above manner to form the monolayer (Fig. 1E). In contrast, the molecules interact with each other weakly along the *a* axis (Fig. 1H), and it is clear that the lamellar structure is formed by means of AB stacking, and the interlayers depend mainly on π–π interactions between the benzene rings in the anionic skeleton. Intramolecular hydrogen bonding between the O atom of the ester group and the H atom of the methyl group in the CIL also occurs within the CIOC framework, but it does not contribute to the overall structure building. It was proved that a novel ionic crystal combining 4,4′-bipyridium-based CIL and BDA was synthesized with ionic bonding as the primary mode of chemical bonding, resulting in an ordered arrangement of atoms.

The scanning electron microscopy (SEM) image confirmed that the CIOC is a macro-sized lamellar stacked solid (Fig. 1A), which is consistent with the SXRD results. The Fourier transform-infrared (FT-IR) spectra (Fig. S3A†) and powder X-ray diffraction (PXRD) pattern (Fig. S3B†) prove the successful synthesis of the CIOC. 2D-NSs with repeating topological units can be obtained from CIOC *via* ultrasonic exfoliation. The FT-IR spectrum and XRD pattern of the 2D-NSs confirmed that the composition and crystal structure remain unchanged (Fig. S3†). The SEM image (Fig. 1B) showed that the exfoliated CIOC was lamellar. The atomic force microscopy (AFM) image revealed lamellae with sharp edges (Fig. 1C), and the height was measured to be about 10 nm (Fig. 1D), which proved that 2D-NSs were successfully prepared. The CIOC is a 2D crystal formed by π–π stacking between different layers, with a distance of approximately 0.5 nm between layers (Fig. 1E). It can be inferred that the 2D-NSs obtained through exfoliation consist of approximately 20 monolayers. High-resolution transmission electron microscopy (HRTEM) revealed well-ordered linear features with a lattice spacing of 0.43 nm (Fig. 1F), demonstrating that the 2D-NSs still maintain good crystalline structure. The selected area electron diffraction (SAED) pattern of the 2D-NSs revealed nearest reflections at 0.14 nm (Fig. 1G), confirming the existence of the crystalline structure of the exfoliated 2D-NSs with regular diffraction points. Fig. S3C† confirms that both the CIL and 2D-NSs are optically active and also reveals the chiral retention of the synthesized nanosheets. The CIL appears as three signal peaks on the circular dichroism (CD) spectrum with a *g*-factor of about 4×10^{-4} (Fig. S3D†). In contrast, both CD signal peaks of the 2D-NSs show a red-shift (Fig. S3E†), and the *g*-factor was also reduced, which might originate from the effect of the BDA.

The N_2 adsorption experiment (Fig. S3F†) demonstrated that both the CIOC and 2D-NSs have a type II isotherm, and the Brunauer–Emmett–Teller (BET) surface area of the 2D-NSs is significantly increased, which suggests that while both the CIOC and 2D-NSs are non-porous structures, the specific surface area is enhanced by the 2D-NSs produced during

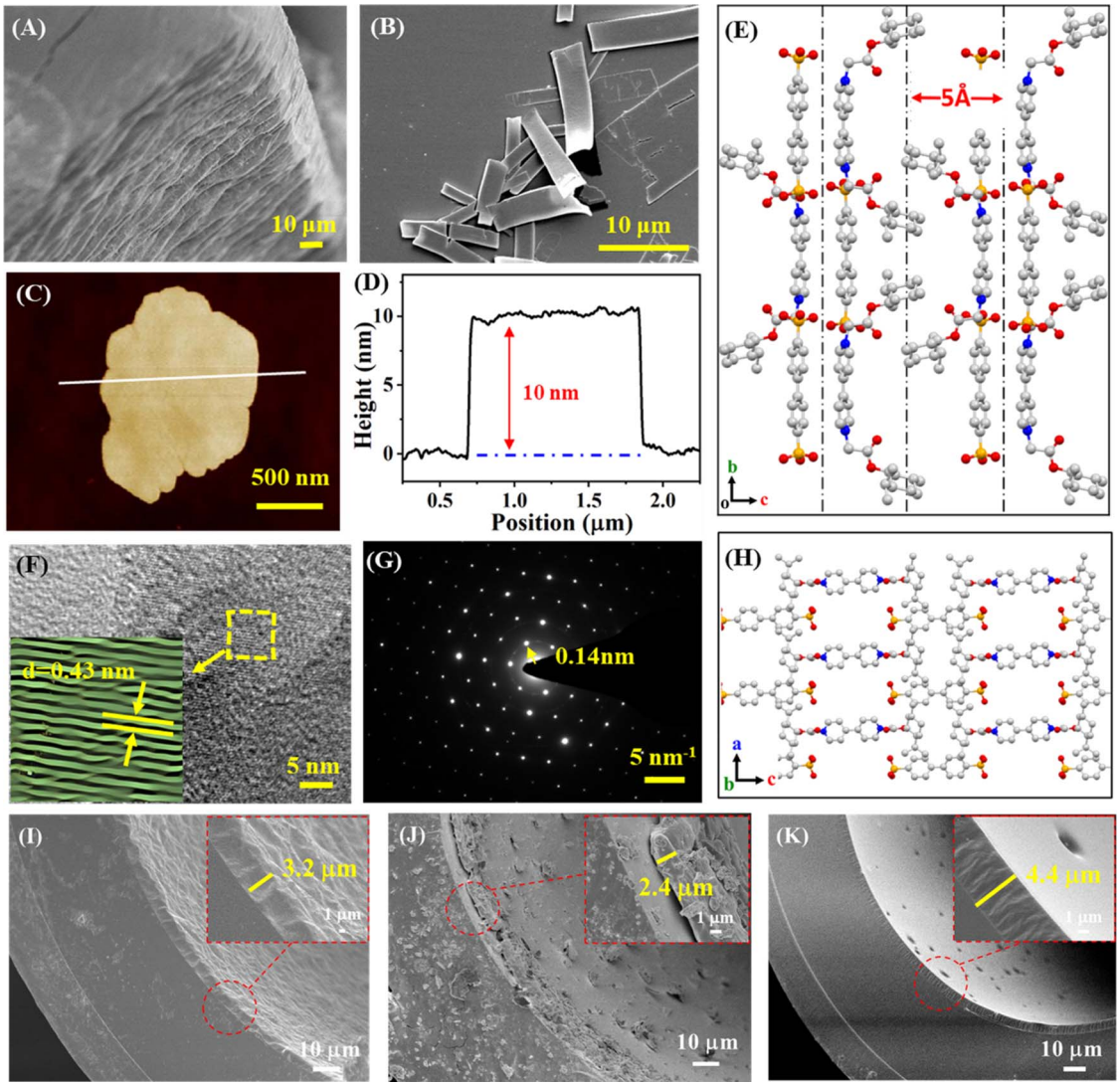

Fig. 1 SEM images of the CIOC (A) and 2D-NSs (B). AFM image of the 2D-NSs (C) and related height analysis (D). Overlapping structure of the CIOC (E). HRTEM image of the 2D-NSs (F). SAED pattern of the 2D-NSs (G). The monolayer structure of the CIOC (H). SEM images showing the cross section of the CIL coated column (I), CIOC coated column (J), and 2D-NSs coated column (K). C: light grey, N: blue, O: red, S: yellow, H is omitted.

exfoliation. Compared to bulk CIOCs, the 2D-NSs expose more interaction sites and have stronger interaction forces with analytes, resulting in a superior selective separation, confirmed by the results of the N_2 adsorption experiment.[50] Thermogravimetric analysis (TGA) showed that the CIL remained stable until the temperature reached 277 °C (Fig. S4A†). In addition, the CIOC and 2D-NSs are thermally stable with the CIL (Fig. S4B and C†); all of them possessed good thermal stability.

Characterizations of capillary columns

SEM images were utilized to show the morphology of the inner wall of the capillary columns. Fig. 1I indicates the successful deposition of the CIL on the inner wall of the capillary with a thickness of 3.2 μm. In Fig. 1J, the inner wall of the capillary column shows the CIOC coating, which has a 2.4 μm coating thickness and takes the shape of lumps with variable sizes. Fig. 1K reveals the presence of protrusions on the surface of the gel layer with sizes of 4.4 μm, confirming the successful preparation of the 2D-NSs coated capillary columns. Fig. S4D† shows that the three proposed columns retain relatively good column stability.

Five probe molecules, including benzene (X′), *n*-butanol (Y′), 2-pentanone (Z′), 1-nitropropane (U′), and pyridine (S′) were used to measure the polarity of the stationary phase using a polarity index.[51,52] The results for the three coated columns showed that they exhibited moderate polarity and were comparable to one another (Table S3†).

Separation of chiral compounds

The separation of chiral compounds has always been a challenging task. In Fig. 2, one pair of *cis*-/*trans*-isomers (decahydronaphthalene) and 3 enantiomers, mandelonitrile,

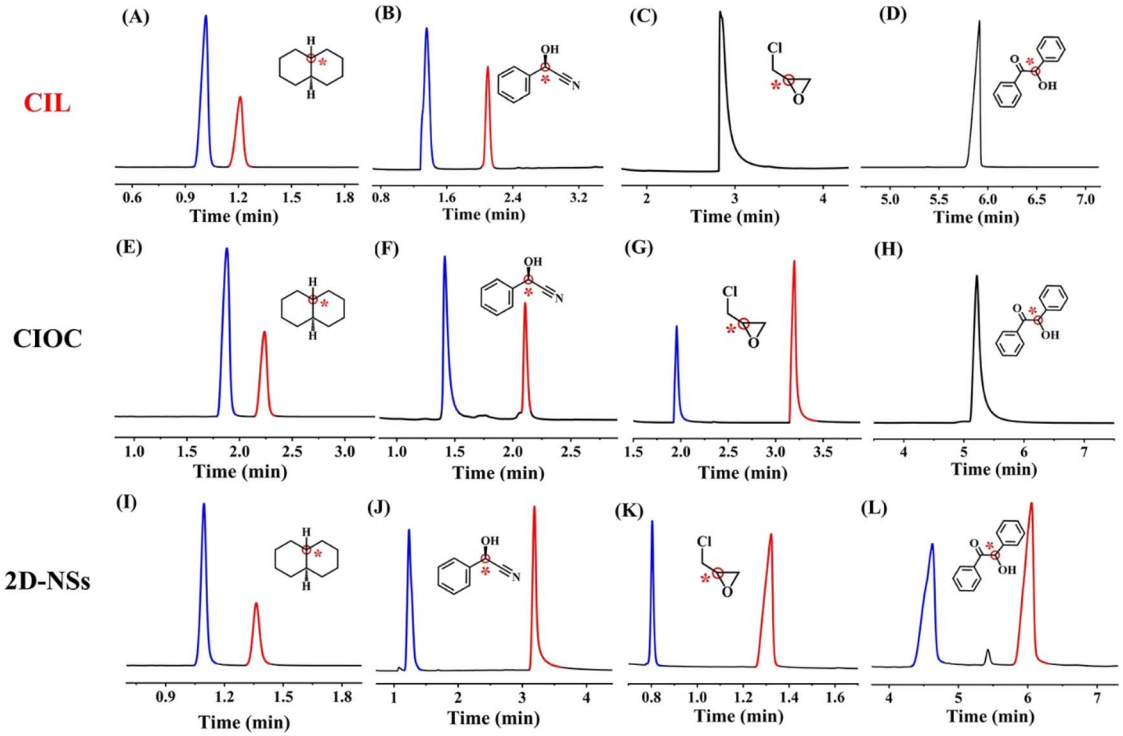

Fig. 2 Representative gas chromatograms for the separation of *cis*-/*trans*-isomers and enantiomers on CIL-/CIOC/2D-NSs-coated columns: decahydronaphthalene (A, E, and I); mandelonitrile (B, F, and J); epichlorohydrin (C, G, and K); and benzoin (D, H, and L). Separation conditions are shown in Tables S4–6.† Derivatization can be found in the ESI.†

epichlorohydrin and benzoin, were separated as test compounds. For decahydronaphthalene and mandelonitrile, the resolution (R_s) and selective factor (α) of the 2D-NSs coated capillary column reached 14.85 and 4.86, and the values for the CIOC coated columns reached 11.00 and 2.99, whereas the values for the CIL coated column were 6.85 and 2.64. The enantiomer separation ability can be reasonably determined to be in the following order: 2D-NSs > CIOC > CIL based on the separation results. This improvement can be attributed to the connection between the CIL and BDA increasing hydrogen bonding, dipole–dipole, and π–π interactions, as well as the introduction of certain steric hindrance effects. Regarding benzoin, the 2D-NSs coated column was able to achieve the baseline separation, whereas the CIOC coated column showed no signs of separation. Compared to bulk CIOC, the 2D-NSs exposed more interaction sites and exhibited stronger interaction forces with analytes, resulting in superior selective separation, confirmed by the results of the N_2 adsorption experiment. Commercialized β-DEX 120 was used to make comparisons, with results such as those in Table S7,† where 2D-NSs coated capillary columns still exhibited enantiomeric separation advantages.

In order to investigate the thermodynamic parameters of the separation on CIL, CIOC and 2D-NSs coated columns, we separated the *cis*-/*trans*-decahydronaphthalene isomers at different temperatures (Fig. S5A–C†). The reduction in retention time and R_s as the temperature increases indicates an exothermic separation process for *cis*-/*trans*-decahydronaphthalene. The relevant Van't Hoff equations (Fig. S5D–F†) showed excellent linearity, confirming that the separation mechanism of *cis*-/*trans*-decahydronaphthalene was not altered. Negative values of the Gibbs free energy change (ΔG) suggest the spontaneity of the separation process, while negative entropy change (ΔS) and enthalpy change (ΔH) values collectively govern the separation process throughout, as shown in Table S8.†

To further elucidate the mechanism of separation and explore the microscopic interaction pattern between chiral compounds and the stationary phase, energy-minimized DFT calculations and relevant NCI studies have been carried out for

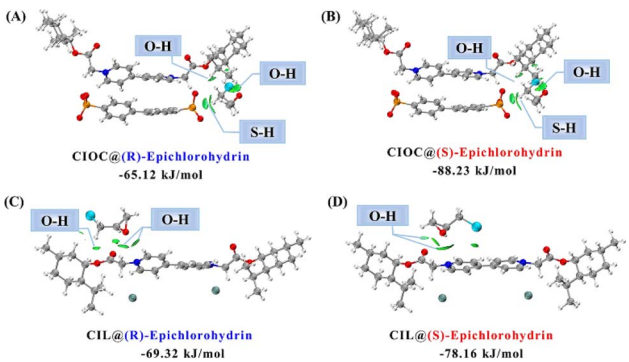

Fig. 3 Energy-minimized DFT and NCI analysis for CIOC@(*R*)-epichlorohydrin (A), CIOC@(*S*)-epichlorohydrin (B), CIL@(*R*)-epichlorohydrin (C), and CIL@(*S*)-epichlorohydrin (D).

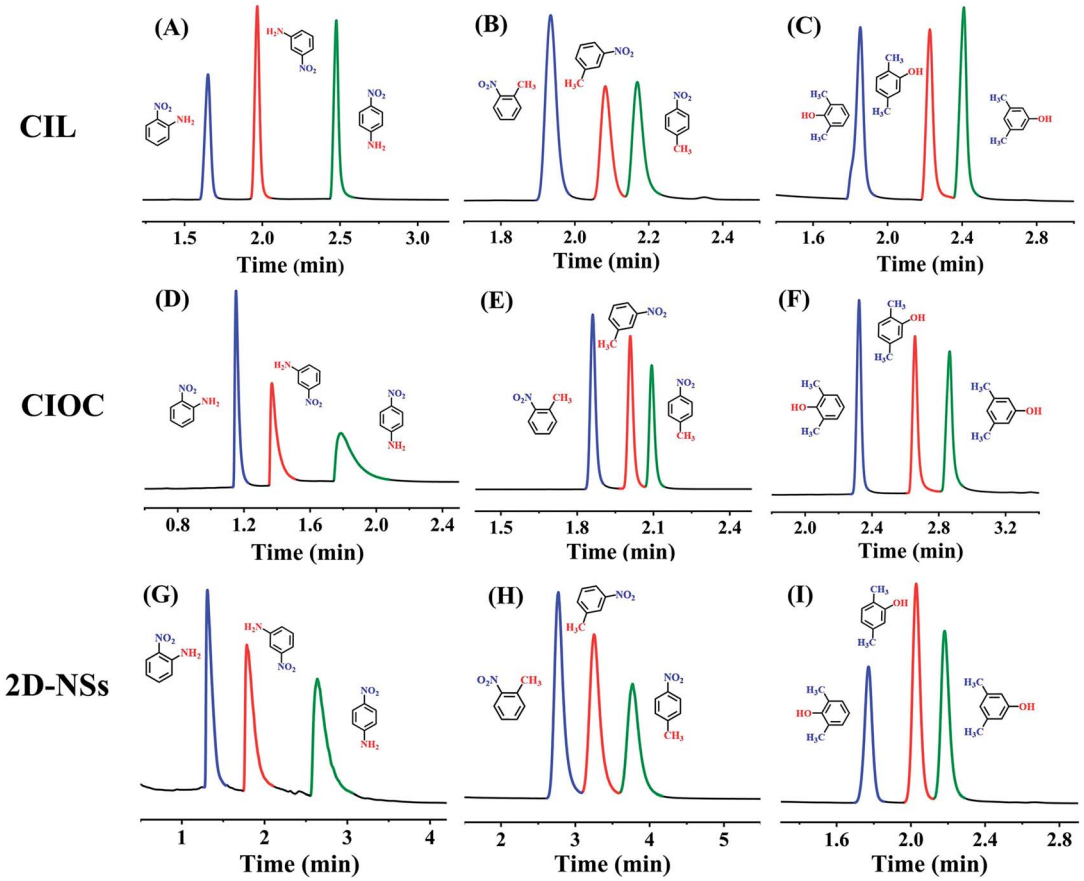

Fig. 4 Gas chromatograms of positional isomers on CIL, CIOC and 2D-NSs coated capillary columns: nitroaniline (A, D, and G), nitrotoluene (B, E, and H), and dimethylphenol (C, F, and I). Oven program: 100–170 °C at 30 °C min^{-1} for (A), 50–150 °C at 30 °C min^{-1} for (B), 70–150 °C at 20 °C min^{-1} for (C), 120–180 °C at 50 °C min^{-1} for (D), 80–140 °C at 30 °C min^{-1} for (E), 100–150 °C at 20 °C min^{-1} for (F, and G), 90–160 °C at 20 °C min^{-1} for (H), and 120–150 °C at 20 °C min^{-1} for (I). Flow rate: 3.0 mL min^{-1} for (A, and B); 2.0 mL min^{-1} for (C, E, and G); 4.0 mL min^{-1} for (D); 1.5 mL min^{-1} for (F); 0.8 mL min^{-1} for (H); and 1.0 mL min^{-1} for (I).

epichlorohydrin molecules with the CIL or CIOC. As shown in Fig. 3A and B, (*R*/*S*)-epichlorohydrin molecules (oxygen and hydrogen atoms) have multiple hydrogen bonding interactions with CIOC (hydrogen and oxygen atoms on the cation and oxygen atoms on the anion), with bond lengths ranging from 2.28–3.05 Å. The binding energy of CIOC@(*S*)-epichlorohydrin was more negative than that of (*R*)-epichlorohydrin, which proved that the interactions between (*R*)-epichlorohydrin and CIOC were stronger, and thus the CIOC had stronger retention of (*S*)-epichlorohydrin, in agreement with the experimental results. Epichlorohydrin could not be separated on the CIL coated column on account of the two conformations of the molecules being combined with CIL through hydrogen bonding with little difference in binding energies and bond distances between 2.62 and 3.00 Å (Fig. 3C and D). The calculations mentioned above proved that the CIOC structure is more favorable for enantiomeric separation since the inclusion of BDA provides additional hydrogen-bonding interactions and increases the difference in binding energies of chiral compounds of different configurations.

Separation of achiral compounds

Positional isomers, serving as crucial intermediates in various fields, play an essential function in production and biology.[53,54] Good separation of the three positional isomers of nitroaniline, nitrotoluene, and dimethylphenol is shown in Fig. 4, and related chromatographic data are shown in Table S9.† The results indicate that the coated columns exhibit separation capabilities for positional isomers that are comparable to the commercial AB-5MS column (Fig. S6†).

These constructed chiral columns not only performed well for chiral and isomer separation, but also performed well in the separation of other non-polar to polar compounds, including *n*-alkanes, *n*-alkanols, Grob mixture, phenols, anilines and benzene derivatives, with the 2D-NSs coated column exhibiting the best separation performance (chromatograms, related chromatographic conditions, R_s and α are shown in Fig. S7–S9 and Table S10†). By investigating the repeatability and stability of the CIL, CIOC and 2D-NSs coated capillary columns using xylenol isomers as models (Fig. S10, and Table S11†), it was found that the 2D-NSs coated column exhibited good results.

Conclusions

In conclusion, a novel chiral ionic organic single-crystal material was rationally designed and creatively prepared. It was formed by self-assembling recrystallization between organic anions and cations. Furthermore, the corresponding 2D-NSs were constructed through ultrasonic exfoliation. Excellent recognition ability and separation selectivity for chiral compounds was obtained using the 2D-NSs coated capillary column, which is due to the presence of more exposed functional interaction sites. In addition, this novel ionic organic single-crystal and 2D-NSs coated capillary column exhibited good separation of positional isomers, Grob mixture, alkylbenzenes, *etc.* This discovery offers a crucial route for the synthesis of novel chiral ionic organic single-crystals *via* ionic self-assembly and related 2D nanomaterials for chiral separation and other potential applications.

Data availability

All the relevant data of this study are available within the manuscript and its ESI.†

Author contributions

Huifeng Liu: experiment, data curation, visualization, investigation, writing – original draft, validation. Yongrui He: investigation, validation. Jia Chen: conceptualization, discussion, supervision, project administration, funding acquisition, writing – review & editing, validation. Xiaoqing Qu: visualization, validation. Jing He: visualization, validation. Xuwei Chen: supervision, validation. Jianhua Wang: visualization, validation. Hongdeng Qiu: conceptualization, supervision, discussion, writing – review & editing, validation. All authors have given approval to the final version of the manuscript.

Conflicts of interest

There are no conflicts to declare.

Acknowledgements

This work was supported by the National Natural Science Foundation of China (22374159), Gansu Province Outstanding youth Foundation (24JRRA042), the "Light of West China" Program from Chinese Academy of Science (xbzg-zdsys-202008), the Youth Innovation Promotion Association CAS (2021420) and Natural Science Foundation of Shandong Province ZR2022QB246. We also want to express our gratitude to Dr Chen Yuan from Sichuan University for his good suggestion.

Notes and references

1 T. Chen, H. Li, X. Shi, J. Imbrogno and D. Zhao, *J. Am. Chem. Soc.*, 2024, **146**, 14433–14438.
2 N. Xu, K. Su, E.-S. M. El-Sayed, Z. Ju and D. Yuan, *Chem. Sci.*, 2022, **13**, 3582–3588.
3 X. Kang, E. R. Stephens, B. M. Spector-Watts, Z. Li, Y. Liu, L. Liu and Y. Cui, *Chem. Sci.*, 2022, **13**, 9811–9832.
4 H. Li, X. Wang, C. Shi, L. Zhao, Z. Li and H. Qiu, *Chin. Chem. Lett.*, 2023, **34**, 107606.
5 C. Zhu, K. Yang, H. Wang, Y. Fang, L. Feng, J. Zhang, Z. Xiao, X. Wu, Y. Li, Y. Fu, W. Zhang, K. Wang and H. Zhou, *ACS Cent. Sci.*, 2022, **8**, 562–570.
6 Y. Huang, H. Zeng, L. Xie, R. Gao, S. Zhou, Q. Liang, X. Zhang, K. Liang, L. Jiang and B. Kong, *J. Am. Chem. Soc.*, 2022, **144**, 13794–13805.
7 S. Zhang, J. Zhou and H. Li, *Angew. Chem., Int. Ed.*, 2022, **61**, e202204012.
8 T. Miyabe, H. Iida, A. Ohnishi and E. Yashima, *Chem. Sci.*, 2012, **3**, 863–867.
9 Y. Cui, C. Yang and X. Yan, *ACS Appl. Mater. Interfaces*, 2020, **12**, 4954–4961.
10 W. Kou, C. Yang and X. Yan, *J. Mater. Chem. A*, 2018, **6**, 17861–17866.
11 Q. Song, J. Yang, K. Zheng, T. Zhang, C. Yuan, L. Yuan and X. Hou, *J. Am. Chem. Soc.*, 2024, **146**, 7594–7604.
12 M. Xu, P. Cai, S. Meng, Y. Yang, D. Zheng, Q. Zhang, L. Gu, H. Zhou and Z. Gu, *Angew. Chem., Int. Ed.*, 2022, **61**, e202207786.
13 J. Chen, Y. Huang, X. Wei, X. Lei, L. Zhao, M. Guan and H. Qiu, *Chem. Commun.*, 2019, **55**, 10908–10911.
14 M. N. Corella-Ochoa, J. B. Tapia, H. N. Rubin, V. Lillo, J. González-Cobos, J. L. Núñez-Rico, S. R. G. Balestra, N. Almora-Barrios, M. Lledós, A. Güell-Bara, J. Cabezas-Giménez, E. C. Escudero-Adán, A. Vidal-Ferran, S. Calero, M. Reynolds, C. Martí-Gastaldo and J. R. Galán-Mascarós, *J. Am. Chem. Soc.*, 2019, **141**, 14306–14316.
15 H. Deng, X. Wu, L. Zhang, J. Shen, Y. Qiao, X. Wang, C. Bai, T. Zheng and Y. Okamoto, *Carbohydr. Polym.*, 2022, **296**, 119888.
16 C. Yuan, W. Jia, Z. Yu, Y. Li, M. Zi, L. Yuan and Y. Cui, *J. Am. Chem. Soc.*, 2022, **144**, 891–900.
17 H. Qian, C. Yang and X. Yan, *Nat. Commun.*, 2016, **7**, 12104.
18 Y. Wang, H. Chen, Y. Xiao, C. H. Ng, T. S. Oh, T. T. Y. Tan and S. C. Ng, *Nat. Protoc.*, 2011, **6**, 935–942.
19 B. Tang, W. Wang, H. Hou, Y. Liu, Z. Liu, L. Geng, L. Sun and A. Luo, *Chin. Chem. Lett.*, 2022, **33**, 898–902.
20 S. Lv, C. Ma, H. Cong, Y. Shen and B. Yu, *Sep. Purif. Technol.*, 2022, **294**, 121147.
21 B. Chankvetadze, *Trends Anal. Chem.*, 2020, **122**, 115709.
22 X. Wang, H. Li, K. Quan, L. Zhao, H. Qiu and Z. Li, *Talanta*, 2021, **225**, 121987.
23 T. Kubota, C. Yamamoto and Y. Okamoto, *J. Am. Chem. Soc.*, 2000, **122**, 4056–4059.
24 L. Dong, J. Xia, H. Song, J. Yang, Y. Sun, X. Li and X. Zhu, *J. Mol. Liq.*, 2023, **371**, 120982.
25 T. Sun, M. Ba, Y. Song, W. Li, Y. Zhang, Z. Cai, S. Hu, X. Liu, D. Nardiello and M. Quinto, *Anal. Chim. Acta*, 2024, **1291**, 342221.
26 C. Shi, H. Li, X. Shi, L. Zhao and H. Qiu, *Chem. Commun.*, 2022, **58**, 3362–3365.
27 Y. Wu, M. Tang, Z. Wang, L. Shi, Z. Xiong, Z. Chen, J. L. Sessler and F. Huang, *Nat. Commun.*, 2023, **14**, 4927.

28 C. Liu, K. Quan, H. Li, X. Shi, J. Chen and H. Qiu, *Chem. Commun.*, 2022, **58**, 13111–13114.
29 C. Yuan, Z. Wang, W. Xiong, Z. Huang, Y. Lai, S. Fu, J. Dong, A. Duan, X. Hou, L. Yuan and Y. Cui, *J. Am. Chem. Soc.*, 2023, **145**, 18956–18967.
30 N. Huang, L. Zhai, D. E. Coupry, M. A. Addicoat, K. Okushita, K. Nishimura, T. Heine and D. Jiang, *Nat. Commun.*, 2016, **7**, 12325.
31 A. A. Kotova, D. Thiebaut, J. Vial, A. Tissot and C. Serre, *Coord. Chem. Rev.*, 2022, **455**, 214364.
32 Y. Wang, J. Chen, L. Xiong, B. Wang, S. Xie, J. Zhang and L. Yuan, *Anal. Chem.*, 2022, **94**, 4961–4969.
33 S. Xie, X. Chen, J. Zhang and L. Yuan, *Trends Anal. Chem.*, 2020, **124**, 115808.
34 X. Han, J. Huang, C. Yuan, Y. Liu and Y. Cui, *J. Am. Chem. Soc.*, 2018, **140**, 892–895.
35 J. Zhang, S. Xie, L. Chen, B. Wang, P. He and L. Yuan, *Anal. Chem.*, 2015, **87**, 7817–7824.
36 A. Kewley, A. Stephenson, L. Chen, M. E. Briggs, T. Hasell and A. I. Cooper, *Chem. Mater.*, 2015, **27**, 3207–3210.
37 J. Xiao, J. Chen, J. Liu, H. Ihara and H. Qiu, *Green Energy Environ.*, 2023, **8**, 1596–1618.
38 J. Chen, Y. Wang, Y. Yu, J. Wang, J. Liu, H. Ihara and H. Qiu, *Exploration*, 2023, **3**, 20220144.
39 K. Dong, X. Liu, H. Dong, X. Zhang and S. Zhang, *Chem. Rev.*, 2017, **117**, 6636–6695.
40 M. Costa Gomes, L. Pison, C. Červinka and A. Padua, *Angew. Chem., Int. Ed.*, 2018, **57**, 11909.
41 Q. Zhao, M. Yin, A. P. Zhang, S. Prescher, M. Antonietti and J. Yuan, *J. Am. Chem. Soc.*, 2013, **135**, 5549–5552.
42 J. Sun, H. Lin, W. Zhang, M. Gao, M. Antonietti and J. Yuan, *Mater. Horiz.*, 2017, **4**, 681–687.
43 J. Ding, T. Welton and D. W. Armstrong, *Anal. Chem.*, 2004, **76**, 6819–6822.
44 H. Liu, J. Chen, M. Chen, J. Wang and H. Qiu, *Anal. Chim. Acta*, 2023, **1274**, 341496.
45 H. Liu, P. Jin, F. Zhu, L. Nie and H. Qiu, *Trends Anal. Chem.*, 2021, **134**, 116132.
46 M. O'Shaughnessy, J. Glover, R. Hafizi, M. Barhi, R. Clowes, S. Y. Chong, S. P. Argent, G. M. Day and A. I. Cooper, *Nature*, 2024, **630**, 102–108.
47 M. Xu, P. Cai, S. S. Meng, Y. Yang, D. S. Zheng, Q. H. Zhang, L. Gu, H. C. Zhou and Z. Y. Gu, *Angew. Chem., Int. Ed.*, 2022, **61**, e202207786.
48 C. Tan, K. Yang, J. Dong, Y. Liu, Y. Liu, J. Jiang and Y. Cui, *J. Am. Chem. Soc.*, 2019, **141**, 17685–17695.
49 J. Dong, L. Liu, C. Tan, Q. Xu, J. Zhang, Z. Qiao, D. Chu, Y. Liu, Q. Zhang, J. Jiang, Y. Han, A. P. Davis and Y. Cui, *Nature*, 2022, **602**, 606–611.
50 J. Guo, Y. Zhang, Y. Zhu, C. Long, M. Zhao, M. He, X. Zhang, J. Lv, B. Han and Z. Tang, *Angew. Chem., Int. Ed.*, 2018, **57**, 6873–6877.
51 T. Ma, W. Deng, H. Qian, S. Xu, C. Yang and X. Yan, *ACS Mater. Lett.*, 2024, **6**, 1616–1622.
52 Z. Wang, C. Yang and X. Yan, *J. Chromatogr. A*, 2019, **1608**, 460420.
53 C. Shi, H. Li, X. Shi, L. Zhao and H. Qiu, *Chin. Chem. Lett.*, 2022, **33**, 3613–3622.
54 B. Huang, K. Li, Q. Ma, T. Xiang, R. Liang, Y. Gong, B. Wang, J. Zhang, S. Xie and L. Yuan, *Anal. Chem.*, 2023, **95**, 13289–13296.